In-Flight Suppression of an Unstable F/A-18 Structural Mode Using the Space Launch System Adaptive Augmenting Control System

Tannen S. VanZwieten * and Eric T. Gilligan †
NASA Marshall Space Flight Center, Huntsville, AL 35812, USA
John H. Wall ‡
Dynamic Concepts, Inc. Huntsville, Alabama 35806, U.S.A.
Christopher J. Miller § and Curtis E. Hanson ¶
NASA Armstrong Flight Research Center, Edwards, CA 93523
Jeb S. Orr ‖
The Charles Stark Draper Laboratory, Inc. Huntsville, AL 35806, USA.

NASA's Space Launch System (SLS) Flight Control System (FCS) includes an Adaptive Augmenting Control (AAC) component which employs a multiplicative gain update law to enhance the performance and robustness of the baseline control system for extreme off-nominal scenarios. The SLS FCS algorithm including AAC has been flight tested utilizing a specially outfitted F/A-18 fighter jet in which the pitch axis control of the aircraft was performed by a Non-linear Dynamic Inversion (NDI) controller, SLS reference models, and the SLS flight software prototype. This paper describes test cases from the research flight campaign in which the fundamental F/A-18 airframe structural mode was identified using post-flight frequency-domain reconstruction, amplified to result in closed loop instability, and suppressed in-flight by the SLS adaptive control system.

I. Introduction

In order to demonstrate the ability of the NASA'S Space Launch System (SLS) adaptive augmenting control (AAC) algorithm described in[1] to recover from or suppress an otherwise unstable structural mode on the physical F/A-18 airframe during the flight test opportunity in,[2] special test cases were performed during the research flights.

The two rounds of flights were required to support the airframe mode recovery objective, as the first collected data for model identification and the second utilized the identification data to produce test cases to challenge the adaptive control with unstable resonance from the physical structure.

During the first flight test, a series of programmed test input (PTI) signals were commanded via existing functionality in the Space Launch System (SLS) flight control system to stimulate and measure the response of the fundamental pitch mode of the 853 airframe. Data measured during the first flight was then used to reconstruct the modal response of the airframe, implement precisely destabilizing filters in the forward control path, and during the second round of research flights demonstrate a closed-loop instability and subsequent recovery with AAC enabled.

*SLS Flight Controls Deputy Lead, Control Systems and Analysis Branch
†Aerospace Engineer, Control Systems and Analysis Branch
‡SLS Flight Controls Deputy Lead, Guidance, Navigation, & Control, (Jacobs ESSSA Group) , AIAA member
§FAST Chief Engineer, Flight Controls & Dynamics Branch
¶Aerospace Engineer, Flight Controls & Dynamics Branch.
‖Sr Member of the Tech Staff, Dynamics & Control, (Jacobs ESSSA Group)

This paper is comprised of three main sections describing the efforts in support of this test: modal identification, amplification test case design, and amplification flight results.

II. Modal Identification

In the production F/A-18 flight control system, a second-order notch filter is applied in the pitch axis control path to provide attenuation of a fundamental structural mode around a frequency of 9.5 Hz (hertz). Figure B-1 shows the notch filter utilized in the F/A-18 pitch axis control system. The same notch filter is placed on the pitch rate feedback in the experiment nonlinear dynamic inversion (NDI) flight control system to preclude any undesirable control-structure interactions. While the notch filter indicated the frequency of a fuselage mode in the launch vehicle adaptive control (LVAC) control path, no additional information on the modal response of the 853 airframe was available at the time of the experiment. To safely and accurately demonstrate an unstable but recoverable (via adaptive control) control-structure interaction, precise identification of the airframe structural response was deemed necessary. The methodology and results of this objective are described in the paragraphs that follow.

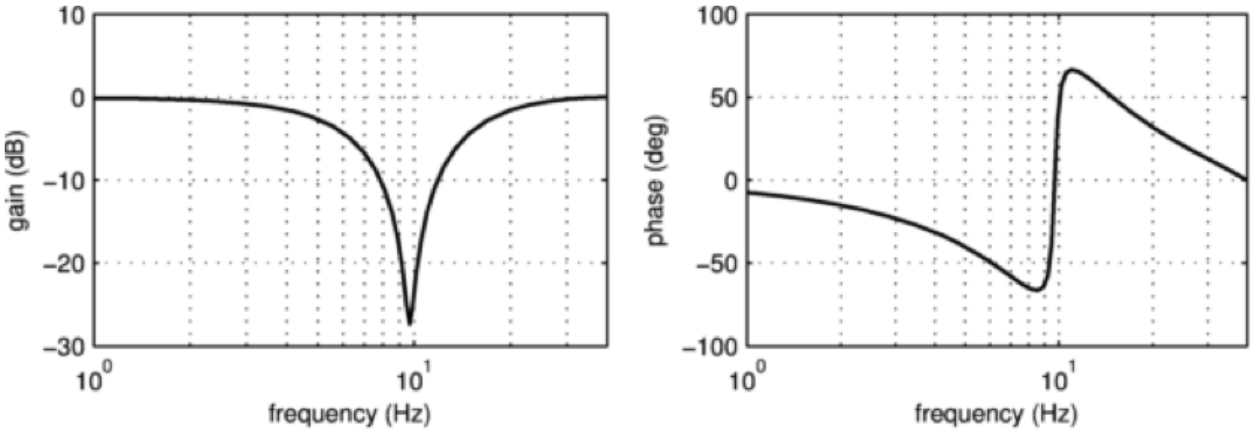

Figure 1. F/A-18 Pitch Axis Notch Filter

For the first flight, a special test case (TC 19) was configured to excite the pitch dynamics of the aircraft over a range of frequencies where the mode was thought to exist. The result from the input excitation measured at the pitch rate feedback was then used to fit a transfer function model of the total system.

To accomplish the excitation, a special programmed test input (PTI) signal was tabulated into existing tables already available for the exact purpose in the SLS controller. Looked up as a function of SLS time, the PTI signal adds a high-frequency waveform to the angular control command prior to the control allocator. Generation of the PTI waveform followed the methodology described in.[3] The PTI signal is a sum of sine waves at a specified number of discrete frequencies whose relative amplitude and phasing is optimized to achieve a particular power distribution over the frequency spectrum and constrain the resultant total waveform amplitude. This approach to modal identification was successfully employed on the Ares I-X flight test and is baselined for the first test flight of the SLS launch vehicle.

The PTI signal employed for the F/A-18 airframe modal identification test was a 20-sec (second) waveform with a frequency range of 8 to 10.5 Hz, a resolution of 0.1 Hz, and a sample rate of 80 Hz, corresponding to the pitch axis controller update rate. The normalized amplitude time signal and the quadratic power weighting profile are shown in Figure 2.

To ensure a sufficiently long window of time for excitation and identification, the 20-sec waveform was concatenated in series three times to produce a 60-sec total waveform. Due to the constraints imposed on the end points of the original 20-sec waveform, the 60-sec version maintained continuity across the concatenation points.

A scalar gain, configurable via presses of the Nose Wheel Steering (NWS) button prior to test point engagement, was applied to the waveform before its injection into the SLS command path. The range of allowable gains allowed for a build-up approach in flight for safety in case the excitation levels were excessive but also permitted the ability to find the largest excitation still within the F/A-18 control surface actuator

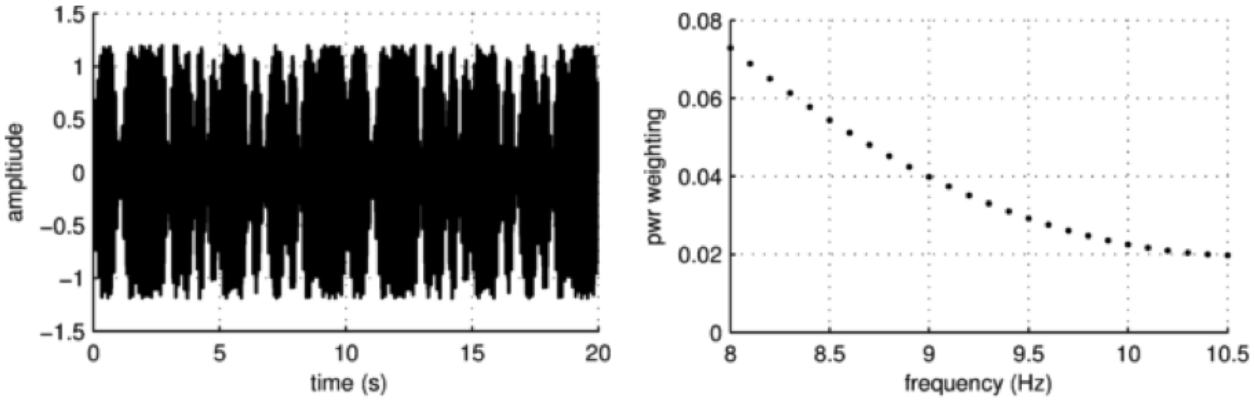

(a) Waveform (b) Weights

Figure 2. PTI Waveform and Power weighting

limits. The objective of the PTI levels in the experiment was to select the largest gain to produce the largest excitation at the fundamental mode frequency still within the linear range (below rate saturation) of the control surfaces. The gains for the excitation waveform corresponding to successive presses of the NWS button are shown in Table II. Large valued PTI gains were required to ensure that excitation of a sufficiently large magnitude was commanded to the control surfaces since the available PTI injection point was prior to the low pass dynamics of the SLS plant model and NDI controller.

Table 1. In-Flight Selectable PTI Gains for TC 19

NWS	PTI Gain
0	5
1	10
2	15
3	20
4	25

Figure 3 shows the overall system block diagram for the first round of research flights during which the modal identification TC 19 was executed. The time-derived PTI signal is shown being added between the SLS FCS and the SLS Optimal Control Allocator (OCA). As was the case with the mainline test cases, the F-18 notch filter was maintained in the NDI feedback but not applied to the SLS feedback. For the mainline cases, this was acceptable since the baseline SLS filters (and plant models) provided sufficient attenuation at 9.5 Hz. For the structural mode test cases, it was desirable to remove the notch filter from the SLS feedback to maximize the gain at 9.5 Hz for the best identification.

While the software architecture for the modal identification experiment was nearly identical to the mainline test cases, several settings were unique to TC 19:

- SLS FCS actuator position and rate limits removed.
- SLS actuator model position and rate limits removed.
- SLS slosh and flex dynamics disabled.
- Guidance command set to fly straight and level (pitch angle and rate = 0) as the rigid body command tracking was not pertinent to the test objective.
- Wind turbulence model disabled.
- NDI control system allocated all control commands to the stabilators (as opposed to mixing with ailerons) to maximize the excitation of the fuselage mode.

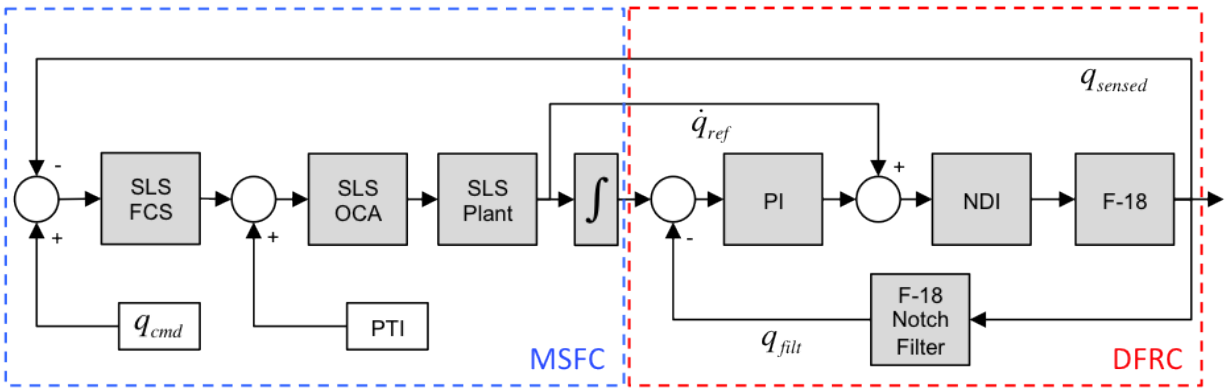

Figure 3. Test Case 19 Implementation Configuration

- Time signal passed into the SLS plant and SLS controller was set to zero to maintain constant parameters in the SLS system.
- SLS FCS rate and attitude filters set to unity.

For the rapid development of test cases at Marshall Space Flight Center (MSFC), the entire Armstrong Flight Research Center (AFRC) NDI control system and F-18 dynamics were approximated with a third-order low pass system with input delay scheduled as a function of flight time along the trajectory. This simplification intended to sufficiently capture the rigid body behavior of the aircraft (up to 2 to 3 Hz) and allowed the MSFC team to quickly build and test stressing SLS scenarios prior to the integration of the MSFC software (SLS FCS and plant models) into the AFRC laboratory environments and eventually flight hardware. MSFC utilized both time-domain models and linear state space models of the entire closed-loop system to develop the test cases. The time-domain models were used to produce time-history results with the time-varying nonlinear SLS plant models, SLS controller, and time-varying linear model of the NDI and F-18 attitude dynamics. The linear state space models were constructed using fixed-time parameters corresponding to the trajectory time and used to assess the stability in the frequency domain via Nichols and Bode plots.

To model the behavior of the airframe structural response around the 8- to 10-Hz range, a simple second-order system with input delay was added to the output of the existing third-order system. By holding the parameters of the existing third-order system constant, the second-order system parameters were used to fit the model to flight data in the frequency range of excitation. The resulting parameters and model form were then used to derive the necessary control filter modifications and simulate the expected behavior in the subsequent flights where the identified mode was intentionally destabilized and recovered with adaptive control. Equation 1 shows the model of the transfer function from the NDI angular acceleration input to the unfiltered pitch rate output.

$$\frac{q_{sensed}}{\dot{q}_{ref}} = \frac{K_R\omega_R^2}{s\left(s^2 + 2\zeta_R\omega_R + \omega_R^2\right)}e^{sT_R} + \frac{K_B\omega_B^2}{s^2 + 2\zeta_B\omega_B + \omega_B^2}e^{sT_B} \tag{1}$$

To determine the parameters for best match, the magnitude and phase of the transfer function from the angular acceleration command into the NDI to the unfiltered sensed pitch rate was compared between the model fit and the flight data. The flight data transfer function was computed by dividing the fast Fourier transform (FFT) of the output over the FFT of the input, after applying a Hann window to the time history data. To efficiently and accurately fit the model parameters to the flight data, a MATLAB optimization routine was written to solve for the natural frequency, damping, and gain that achieved the best match to the flight data. The objective for the optimization routine sought to minimize frequency integral of the squared error of the difference in Bode magnitude between the flight data and the model. The time delay, having no effect on the magnitude response, was then manually tuned to best align the phase responses.

The 853 experiment platform includes two main inertial sensor packages available to the Airborne Research Test System (ARTS) software. The inertial navigation system (INS) sensor package is used as the main sensor for feedback stabilization in both the production and baseline experiment control system and

is mounted near the center of the fuselage. The EGI (Embedded GPS INS) sensor, located farther forward, is an auxiliary sensor providing the same data but is not used in any of the baseline critical functions. The control input for the airframe modal experiments is shown by the arrow at the rear of the aircraft, where a force in the pitch plane is provided by deflection of the stabilators. The stabilators were allocated as the sole means of pitch control input to maximize the excitation of the structure, being located at the rear of the fuselage. Though not considered until after the first test flight (FLT 140), the EGI sensor output was obtained from the telemetry, and identification of its transfer function was pursued alongside the baseline INS. The EGI, being farther forward, gave some promise of having a higher gain at the first mode frequency and, therefore, being more readily destabilized.

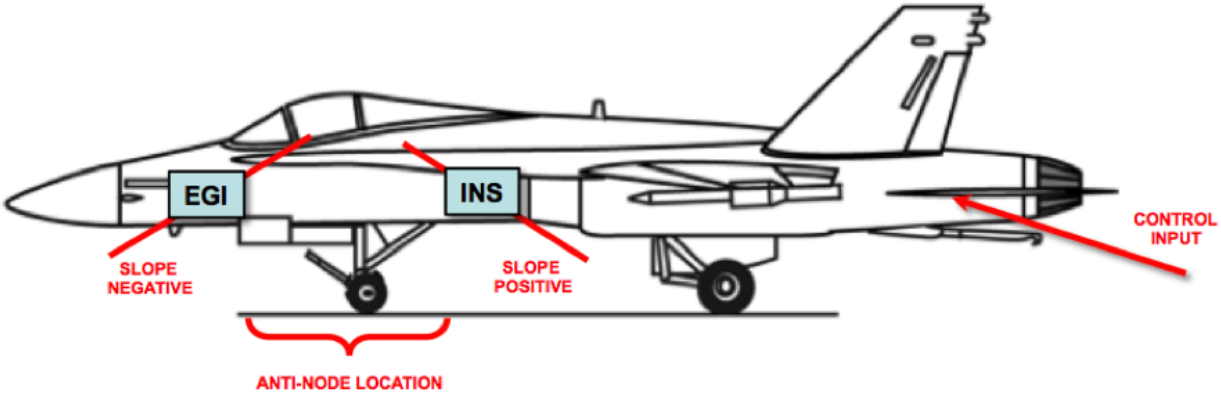

Figure 4. Airframe Sensors and Control Input

At the beginning of the first flight test (FT 140), the pilot maintained straight-and-level flight at particular speed and altitude conditions to achieve a constant dynamic pressure. The pilot then engaged the identification experiment (card 4), with the specified number of NWS button presses, and would maintain the altitude and speed with gentle stick (pitch) and throttle motions. Three such test points were flown in succession for the 60-sec duration with two (15), three (20), and four (25) NWS steering presses. The data shown in the remainder of this section are derived from the 20 NWS presses, but similar results were obtained with using the 15 and 25 test points.

The parameters resulting from the identification of the INS and EGI transfer functions are shown in the last two columns of Table II. These structural mode parameters fit the transfer function model of the response, with the existing rigid body parameters held at constant (t = 0) values (shown here in the first column). Of interesting note is the sign of the gain on the two sensors. With respect to the stabilator command input, the sign of the INS is positive, where the sign of the EGI sensor is negative, with slightly higher gain. Shown pictorially in Figure 4, this indicates that for a presumed first pitch fuselage bending mode shape with a single anti-node, the anti-node falls somewhere between the INS and EGI sensors, with the EGI sensor being somewhat further from the anti-node than the INS. A single 80-Hz frame delay was necessary to model the behavior of the EGI sensor, but no frame delays were required to get acceptable phase matching with the baseline INS sensor.

Table 2. Identified Parameters for Model of Airframe Structural Mode

	Rigid Body (T=0)	INS	EGI
gain	1.0	5.33E-05	-1.24E-04
frequency (Hz)	3.36	9.53	9.41
damping ratio	0.600	0.0411	0.0348
delay (s)	0.044	0	0.0125

Figure 5 shows the raw and windowed time history data of the pitch acceleration input into the NDI and the unfiltered pitch rate from the INS sensor.

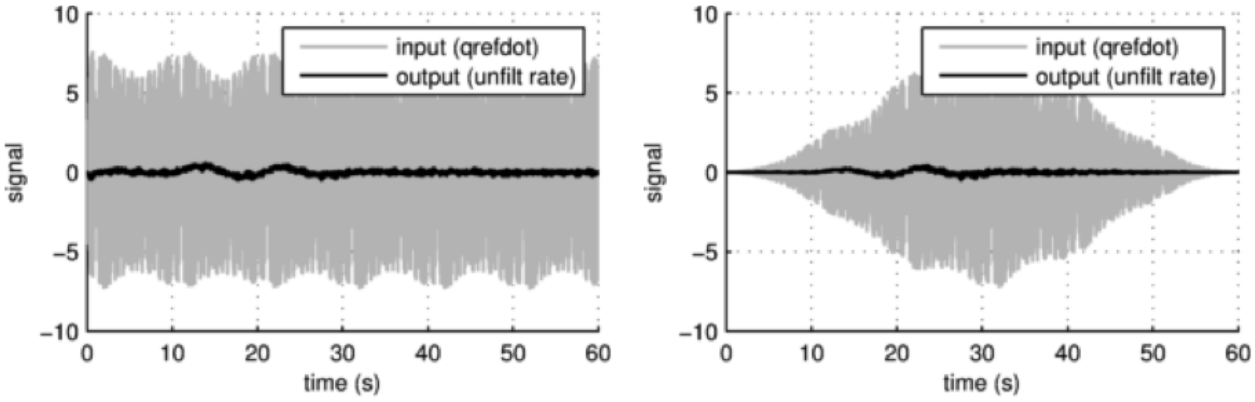

Figure 5. Raw and Windowed Time History of INS

Figure 6 shows the resulting INS sensor frequency response magnitude and phase of the flight data (fft), flight data after 11 point moving average smoothing (fft smoothed), and the model fit (model). A relatively close agreement is achieved with the model parameters being especially visually evident with the smoothed data.

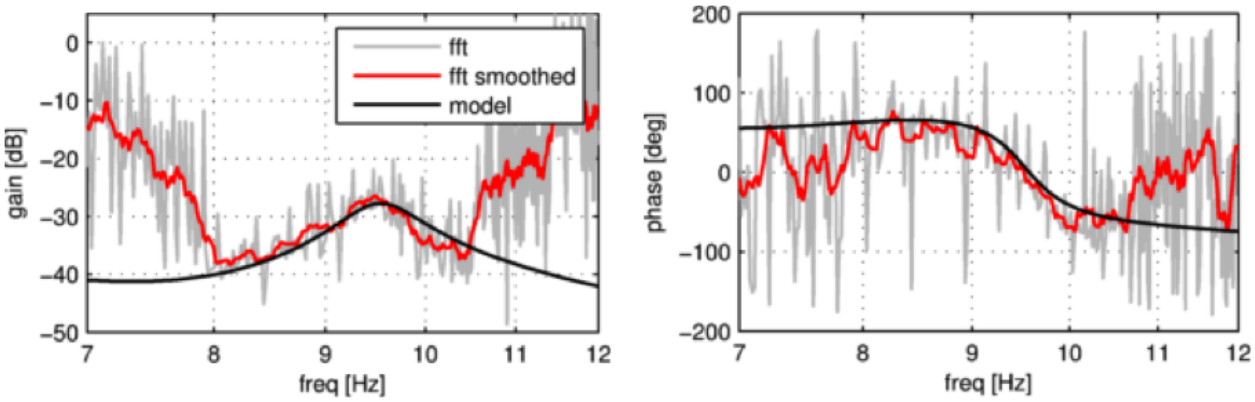

Figure 6. Frequency Response and Model Fit for INS

III. Amplification Test Case Design

After fitting the model for the response of the airframe structural mode to the flight data, TC 20 and TC 22 were created to intentionally set up an unstable control-structure interaction and demonstrate the ability of the AAC algorithm to recover the instability using the INS and EGI sensors, respectively. Filters, gains, and in-flight adjustable frame delays were applied to the control path to bring the mode to a precise amount of instability such that adaptive control had the authority (gain range) to recover. This section describes the development and setup for the amplification TCs 20 and 22.

Figure 7 shows the block diagram configuration for the modal identification experiments TC 20 and TC 22. In contrast to the identification experiment (TC 19), the SLS OCA and plant dynamics were bypassed in TCs 20 and 22, such that the SLS control system angular acceleration command directly input into to the NDI control system. Bypassing the plant dynamics eliminated the irrelevant SLS plant actuator dynamics in the control path and avoided having to produce the additional amplification required to uncover the resultant attenuation at the structural mode frequency. In order to achieve amplification of the airframe mode in the control path, an eighth-order bandpass filter was applied to the output of the SLS FCS along with an adjustable DC gain and frame delay. The selectable frame delays are shown in Table III, and Table III gives the test card options for selecting the various gain levels for each of the two amplification test cases. Note that in the implementation of both sensor feedback configurations, the attitude feedback was

taken from the INS sensor. As the response of the structural mode in the control path at around 9.5 Hz is dominated by the pitch rate, this was an acceptable approach.

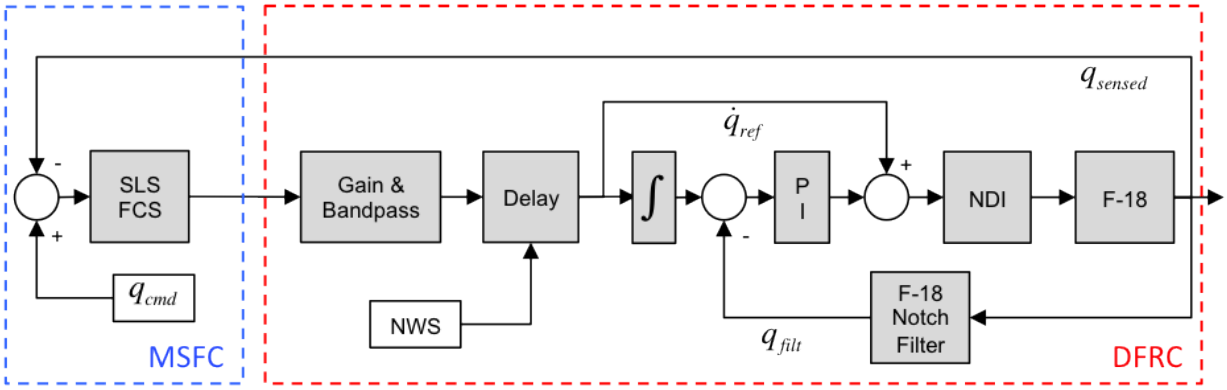

Figure 7. Amplification Experiment Configuration

Table 3. In-Flight Frame Delays for TC20 and TC22

NWS	Frame Delay	Phase Delay 9.5 Hertz
0	0 (0.0000 s)	00.00 deg
1	1 (0.0125 s)	42.75 deg
2	2 (0.0250 s)	85.50 deg
3	3 (0.0375 s)	128.25 deg
4	4 (0.0500 s)	171.00 deg

Table 4. Test Cards for Amplification Cases TC20 and TC22

Test Case	Gain	Card Number
20	-3 dB	43
	0 dB	44
	+3 dB	45
	+6 dB	46
22	-3 dB	47
	0 dB	48
	+3 dB	49
	+6 dB	50

The originally proposed approach to implement the bandpass filter in the SLS controller rate channel was reconsidered during testing, as filtering at this point in the control path would amplify sensor noise prior to the AAC, causing it to be difficult to discern whether an adaptation would be driven by amplified sensor noise or actual structural resonance. Applying the bandpass filter after the SLS controller achieves equivalent control path amplification without gaining-up sensor noise going into the AAC spectral damper.

To ensure excitation of the modal dynamics in the otherwise quiescent straight and level flight, a short, 2-sec burst of the original PTI maneuver from TC 19 was added to the control command signal. The PTI gain was decreased to a magnitude of 0.1, a value determined from simulation sufficient to excite the modeled structural mode but without inducing significant rigid body motion or control effort.

The settings for the modal amplification TC 20 and TC 22 depart from the mainline test cases in the same respects as the modal identification TC 19 and include the following additional modifications:

- SLS OCA and plant bypassed in SLS reference model by connecting SLS flight control system angular acceleration command directly to F-18 NDI control system.
- Gain, delay, and bandpass filter applied to SLS control system output in ARTS software.
- PTI maneuver time-cropped and de-weighted to induce a small excitation for a short, 2-sec burst at 5 sec after the experiment engaged.

A. Modal Amplification with INS sensor

To determine the amount of amplification and phasing required by the bandpass filter for each of the test cases, the modal identification model fit parameters were installed with a unity bandpass filter, and the entire open-loop frequency response was generated. The open-loop frequency response is defined from the input into the NDI to the output of the SLS FCS, the Single-Input-Single-Output (SISO) point where the bandpass filter, gain, and delay is to be applied. Figure 8 shows the open-loop bode response when using the INS sensor for pitch rate feedback

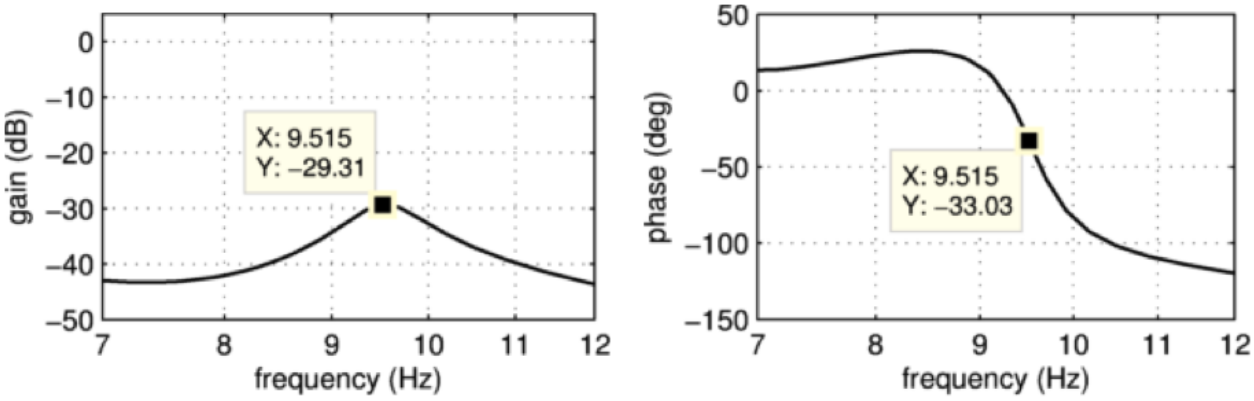

Figure 8. Open-Loop Response without Bandpass: INS feedback

The open-loop response at the peak is at approximately -29 dB of gain and -33 deg of phase. To bring the mode to instability, the required amplification is at least 29 dB and 180 - 33 = 147 deg of phase lag. Initial attempts to design an eighth-order bandpass filter that simultaneously met the gain and phase objectives proved difficult. To alleviate the phase constraints on the filter, a number of discrete frame delays were added to the path. Utilizing two 80 Hz frame delays (selectable via NWS presses in flight) provides 85.5 deg of phase lag at 9.5 Hz, which leaves 61.5 deg to be achieved with the filter.

The filter was designed utilizing the standalone filter optimization tool in the MSFC control parameter design and frequency domain stability analysis tool, FRACTAL. The methodology of the FRACTAL filter optimization tool is described in reference.[4] To achieve the desired 29 deg of gain and 61.5 deg of phase lag at 9.5 Hz, gain targets and phase constraints were configured in the filter design tool and run to solve for the eighth-order set of coefficients to best achieve the objectives. Figure 9 shows the frequency response of the resultant filter against the magnitude targets (shaded areas) and phase constraints (red pluses). The filter amplitude and phase at the mode frequency was designed to achieve the very precise targets. At frequencies lower than the passband centered 9.5 Hz, the filter was specified to have unity DC gain so as to not affect the basic rigid body response or stability characteristics. At frequencies higher than the 9.5 Hz passband, attenuation is beneficial to filter out noise or any other irrelevant dynamics.

After placing the bandpass filter in the control path and computing the open-loop response, the open-loop gain at the mode frequency is slightly above unity, but the phase lag is still 80 deg from the critical -180 degree phase point, as the filter is nearly fully constrained by the gain objectives. However, this is easily remedied by selecting two 80-Hz frame delays in flight to increase the lag to 108 + 85.5 = 193.5 deg. To further ensure an unstable mode in flight given the potential uncertainty, the test card was selected that added an additional +3 dB of gain to the control path. These two adjustments along with the filter placed the open-loop response of the airframe mode at a predicted +3.3 dB and 193.5 deg. Given the AAC gain range from -6 dB to +6 dB, the response of the system with the adjustments would have enough gain

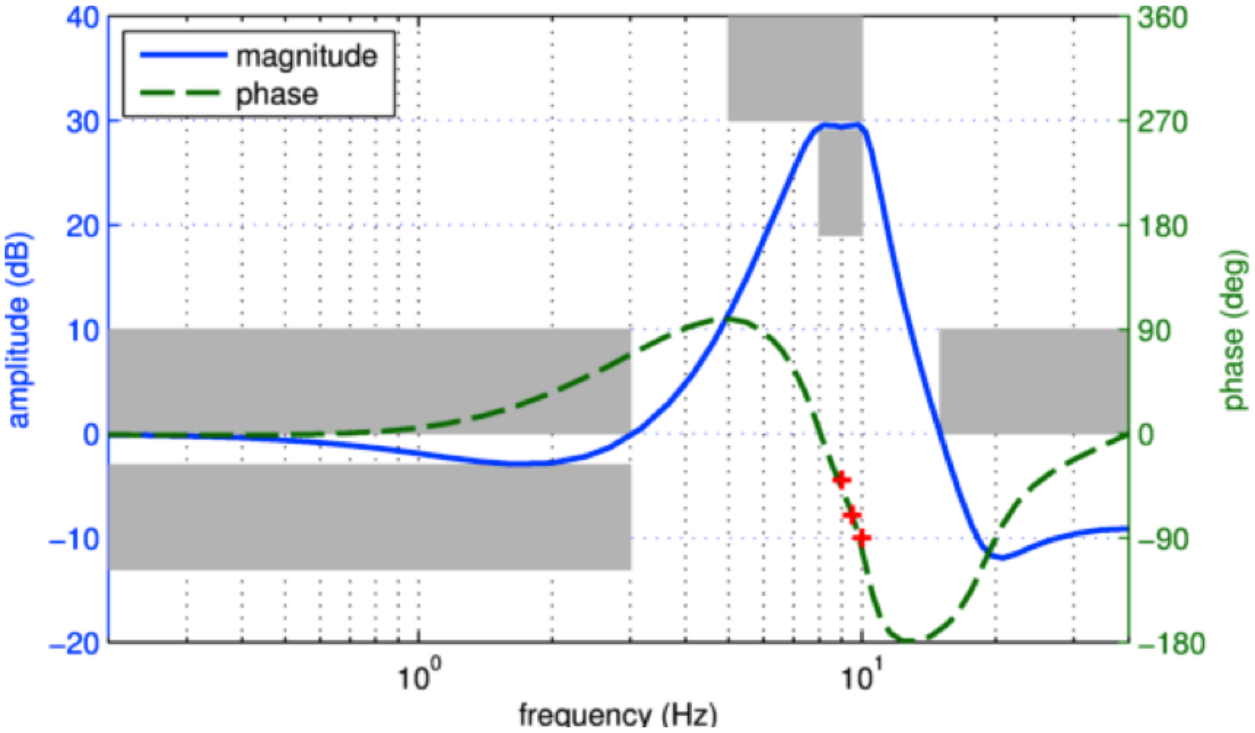

Figure 9. Bandpass Filter Response and Specifications: INS Feedback

to exhibit divergence but not too much gain that AAC would be unable to decrease its gain to restore stability. Furthermore, due to the higher level of damping (4 %) of the structural mode (compared with the SLS assumed 0.5 %), the resultant gain at 180 deg for a moderate phase variation remains above 0 dB and, therefore, would result in a divergent response. In the case where the gain or phase of the mode was mismodeled or the response is higher than expected, the in-flight selectable gains and delays allowed some additional flexibility (subject to flight time constraints) toward finding the instability.

Figure 10 shows the final system as configured for test flight in which two frame delays are selected for the +3 dB test card.

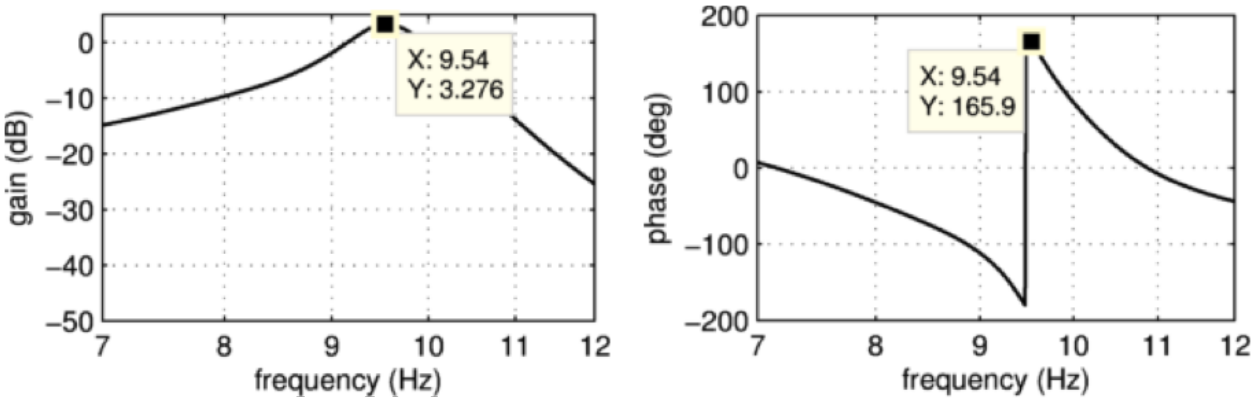

Figure 10. Open-loop Response with Bandpass Filter, Gain, and Delays Applied: INS Feedback

Figure 11 shows a Nichols chart of the open-loop response with the 3-dB gain and two frame delays configured. This depiction best illustrates the gain versus phase relationship resulting from the 4 % modal response near the critical point: even though the magnitude peak of the frequency response does not exhibit exactly -180-deg phase (14 deg away), there is still sufficient gain at the -540 phase point to produce an instability. The Nichols plot also shows the adequate rigid body margins present in this test case configuration,

even after the application of in-flight gain and phase adjustments.

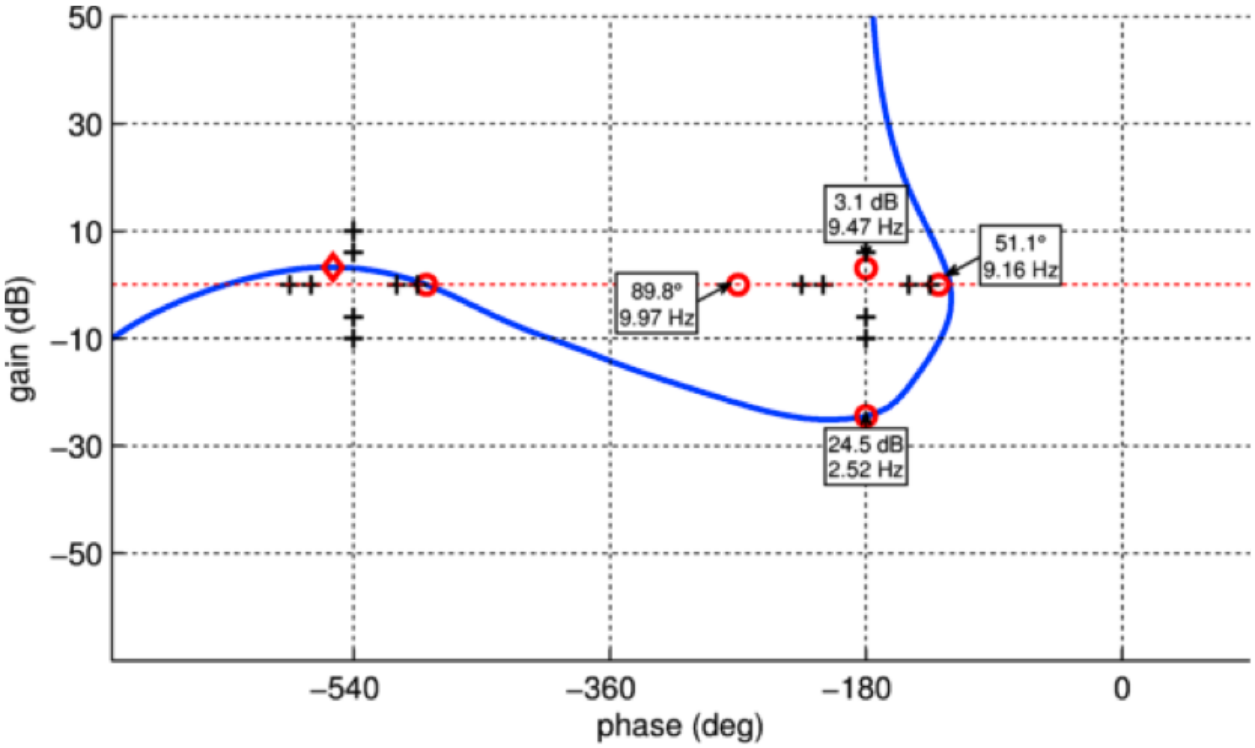

Figure 11. Nichols Open-loop Response with Bandpass Filter, Gain, and Delays Applied: INS feedback

Time domain results generated using the MSFC simulation for TC 20, corresponding to the +3-dB gain and two frame delay settings, are shown in Figure 12. The AAC-off (gray line) case, once hit by the short 0.1-gained PTI burst at 5 sec, exhibits an immediately divergent oscillation that grows until eventually reaching the limit of the numerical simulation. The left plots in Figure 12 show that when AAC is enabled the control command and pitch rate are bounded and exhibit stable behavior. The total gain (bottom right) profile, while periodic, suppresses the unstable mode by decreasing the gain and subsequently preventing divergence. The gain law also nears the lower limit and exhibits the predicted saturation behavior. The gain law input terms are shown in the upper right plot of Figure 12, demonstrating the activity of the spectral damper (sdamp) driving the gain down while the leakage term attracts the gain back to unity. The peaking in the spectral damper is expected due to the sudden decrease of the saturation function when the gain nears its lower limit. Since no physical limits are modeled in the MSFC simulation for this test case, the AAC-off behavior is virtually unbounded. In actual flight, the unstable mode was expected to grow until reaching the physical limitation of the actuators (to an extent not predicted prior to flight), at which point a limit cycling behavior was thought to be likely. By contrast, the AAC-on cases stay within physical limits and were expected to show similar behavior to the preflight simulations.

IV. Amplification Flight Results

As each of the structural mode amplification test cases were flown straight and level for approximately 60 sec, it was straightforward and desirable to fly those test cases when going out or returning home or when the pilot was required to fly to different parts of the available airspace to avoid traffic. This approach maximized achieved test points by utilizing otherwise unusable flight time, at the cost of placing the amplification test points further from the fuel level conditions corresponding to the identification test. Table IV summarizes all of the test cases flown for the modal identification and amplification experiment, along with the fuel remaining, altitude, and speed conditions when the test card was engaged.

The first test engaged during Flight 143 was TC 20, where the airframe structural mode was amplified with INS feedback. The conditions for the gain and delay were set to the +3-dB and two-frame-delay values

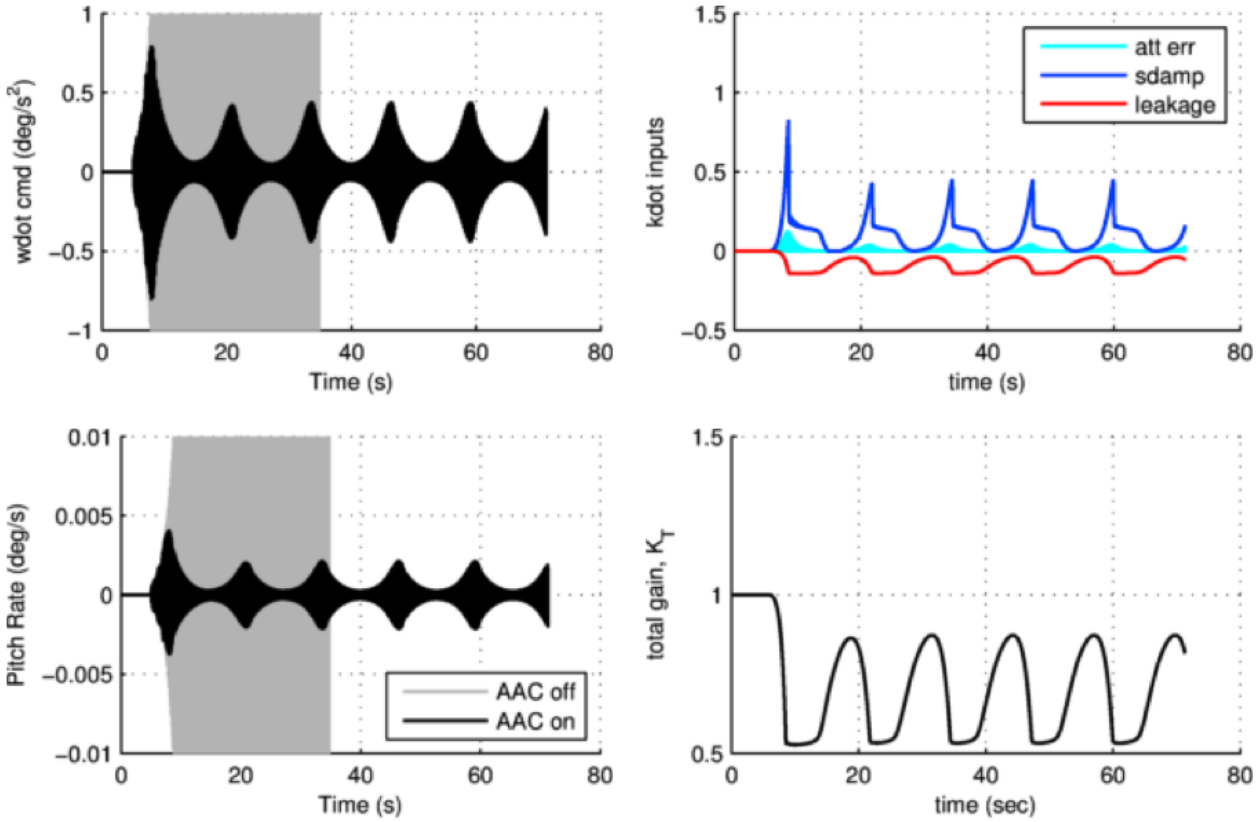

Figure 12. TC20 Simulated Time-Domain Results

Table 5. Test Flight Summary

CASE	FLIGHT	CARD	AAC	GAIN	NWS	FUEL (LB)	ALT (FEET)	MACH
19	140	4	OFF	15	2	8,311	19,005	0.5132
	140	4	OFF	20	3	8,077	18,930	0.5199
	140	4	OFF	25	4	7,887	18,942	0.5198
20	143	45	OFF	+3 dB	2	7,238	18,981	0.5237
	143	49	ON	+3 dB	2	7,125	19,031	0.5162
22	143	53	OFF	+3 dB	3	2,855	18,963	0.5236
	143	54	OFF	+6 dB	3	2,762	19,081	0.5154
22	144	54	OFF	+6 dB	3	6,149	18,874	0.5107
	144	54	OFF	+6 dB	4	6,040	18,911	0.5140
	144	54	OFF	+6 dB	2	6,000	19,072	0.5138
	144	54	OFF	+6 dB	1	5,940	19,047	0.5194
	144	58	ON	+6 dB	1	5,790	19,085	0.5177
	144	58	ON	+6 dB	2	5,565	19,131	0.5260
20	144	45	OFF	+3 dB	2	3,012	19,194	0.5210
	144	49	ON	+3 dB	2	2,875	19,137	0.5208
	144	46	OFF	+6 dB	2	2,682	18,976	0.5122

predicted in preflight simulation to bring the mode to a recoverable level of instability. The first test point was engaged with AAC off and soon after the PTI burst at 5 sec; a fast growth to bounded oscillation was observed in the symmetric stabilator commands. This, along with a distinct 9.5-Hz peak in the real-time PSD displays, demonstrated that the resultant system response at the predicted structural mode frequency was unstable. The presence of the stabilator rate limit and possibly other amplitude-dependent mechanisms of energy dissipation maintained the system response to a stable limit cycle at the resonant frequency of the airframe, and the pilot confirmed a detectable vibration in the cockpit. TC 20 was then engaged for the same conditions but with the AAC enabled. The symmetric stabilator command grew quickly to oscillation after the PTI burst, but the magnitude of oscillations thereafter continued to be suppressed by the action of the adaptive controller and were significantly less than when AAC was disabled. The total loop gain, in the presence of the airframe structural mode excitation, continued to be adjusted by the adaptive controller to suppress the otherwise unstable mode.

Figure 13 shows the results of TC 20 with AAC off and AAC on during Flight 143. The gray line in the upper left plot demonstrates the saturated state of the stabilator command due to limiting in the stabilator actuator system. The black line indicates the suppressed value of the stabilator command, as arrested by the decrease of total loop gain below unity shown in the bottom right plot. The upper left plot shows the spectral damper input to the first order adaptive law sdamp continuing to arrest the growth of the mode in the control path. The oscillatory behavior of the adaptation response shown follows the trend as simulated prior to test (Figure 12) although the gain does not appear to decrease to the same extent. The difference in gain behavior may be due to the fact that the severity of the instability in flight may be less than predicted based upon the model fit or nonlinear behavior of the actuators near their maximum capability.

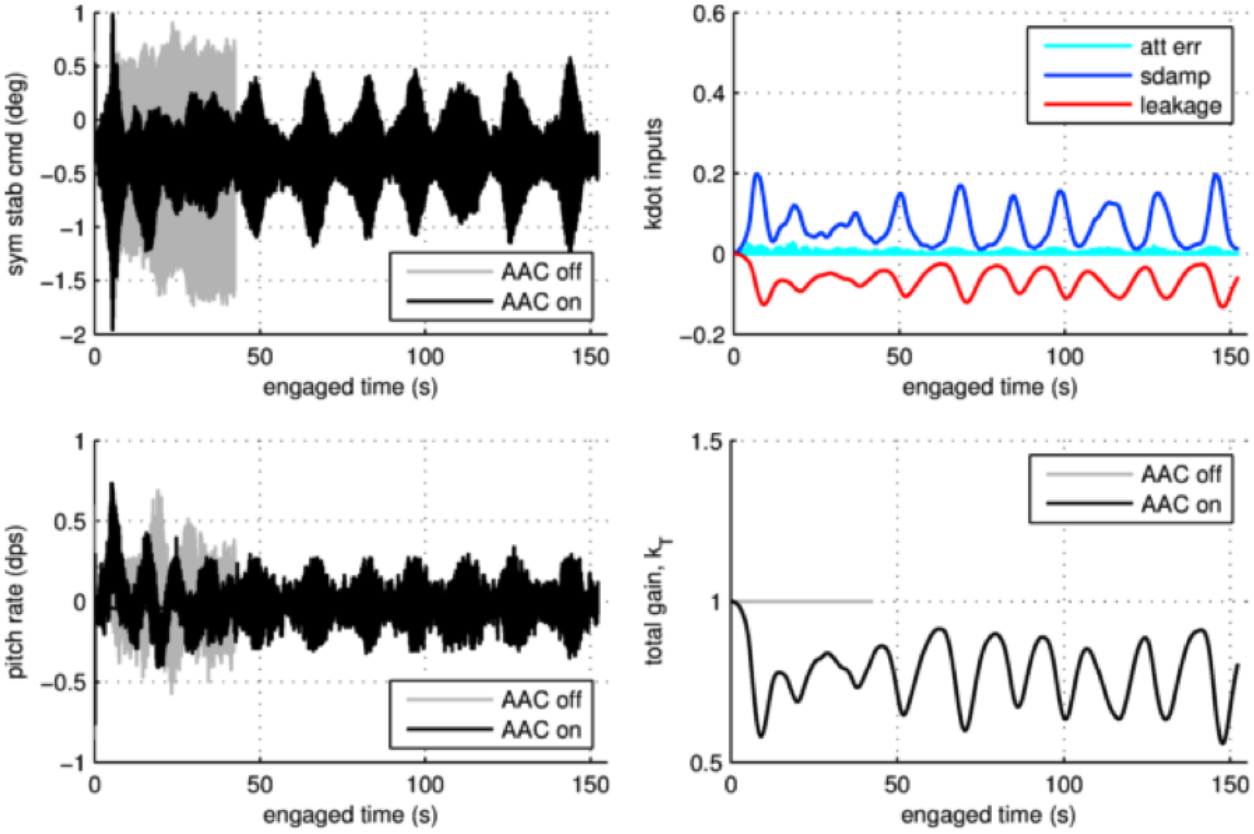

Figure 13. Test Case 20 Flight 143 Results

Figure 14 shows the results of TC 20 as flown at the very end of Flight 144. Despite being engaged with the exact same gain and phase settings as in Flight 143, the amplitude of the stabilator response is less for Flight 144. The adaptive gain decreases in response to the excitation, but to a lesser extent, indicating that the mode is either stable or is less unstable than in the FLT 143 test point.

Figure 15 shows the altitude, speed, and fuel level conditions for identification TC 19 and TC 20 runs in

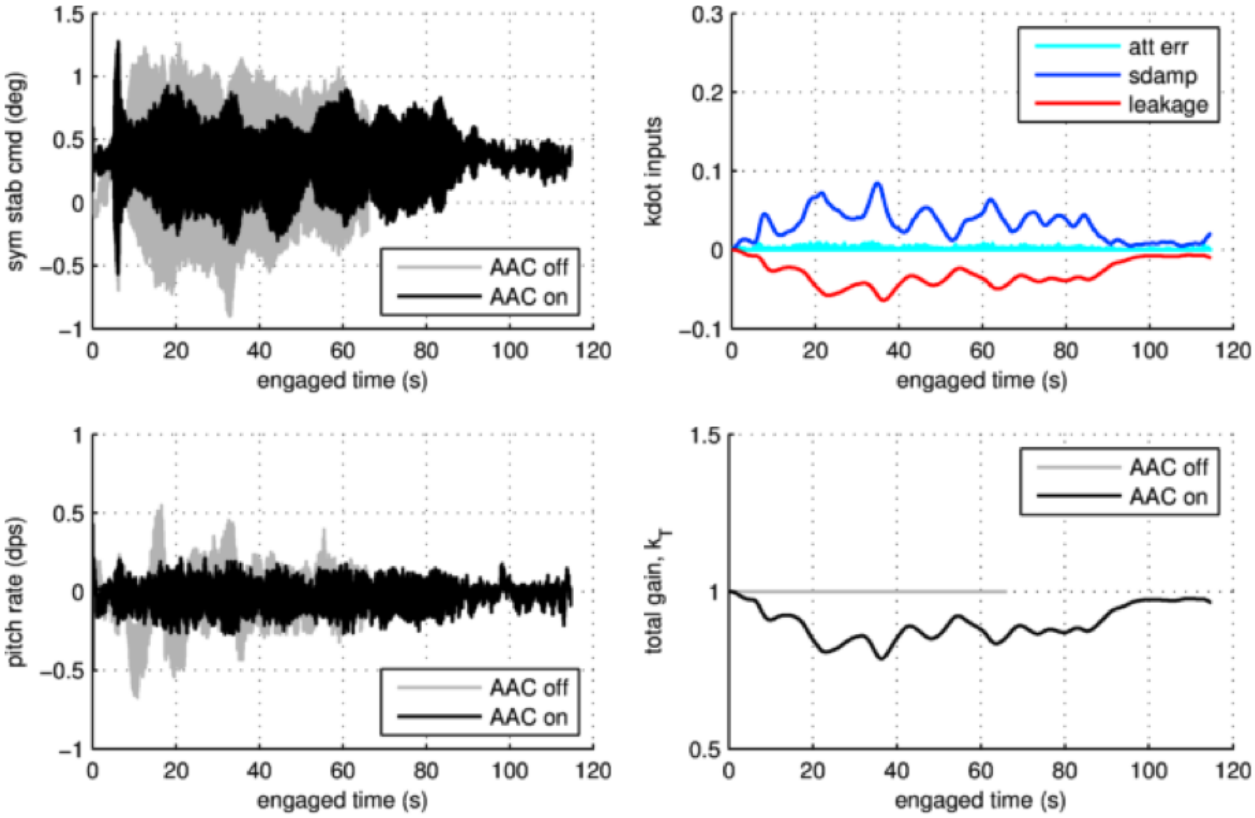

Figure 14. Test Case 20 Flight 144 Results

both Flight 143 and 144. While the altitude and speed conditions are all within variation of each other, the fuel level in Flight 144, being executed at the end of the research flight, is significantly further away from the conditions used to identify the modal response (TC 19 flown at the beginning of research Flight 140). The fuel-level condition, since it affects the total mass and mass distribution of the vehicle and, therefore, the structural dynamic characteristics, is the probable cause of the degraded performance for TC 20 in Flight 144.

References

[1]Wall, J., Orr, J., and VanZwieten, T., "Space Launch System Implementation of Adaptive Augmenting Control," American Astronautical Society Guidance, Navigation, and Control Conference, Breckenridge, Colorado, Jan 31-Feb 5, 2014, AAS 14-051.

[2]VanZwieten, T., Gilligan, E., Wall, J., Orr, J., Miller, C., and Hanson, C., "Adaptive Augmenting Control Flight Characterization Experiment on an F/A-18," American Astronautical Society Guidance, Navigation, and Control Conference, Breckenridge, Colorado, Jan 31-Feb 5, 2014, AAS 14-052.

[3]Morelli, E. A., "Multiple Input Design for Real-time Parameter Estimation in the Frequency Domain," Paper REG-360, 13th IFAC Symposium on System Identification, Rotterdam, The Netherlands, August 2003.

[4]Orr, J., "Optimal Recursive Digital Filters for Active Bending Stabilization," AAS Guidance, Navigation, and Control Conference, Breckenridge, CO, 2013.

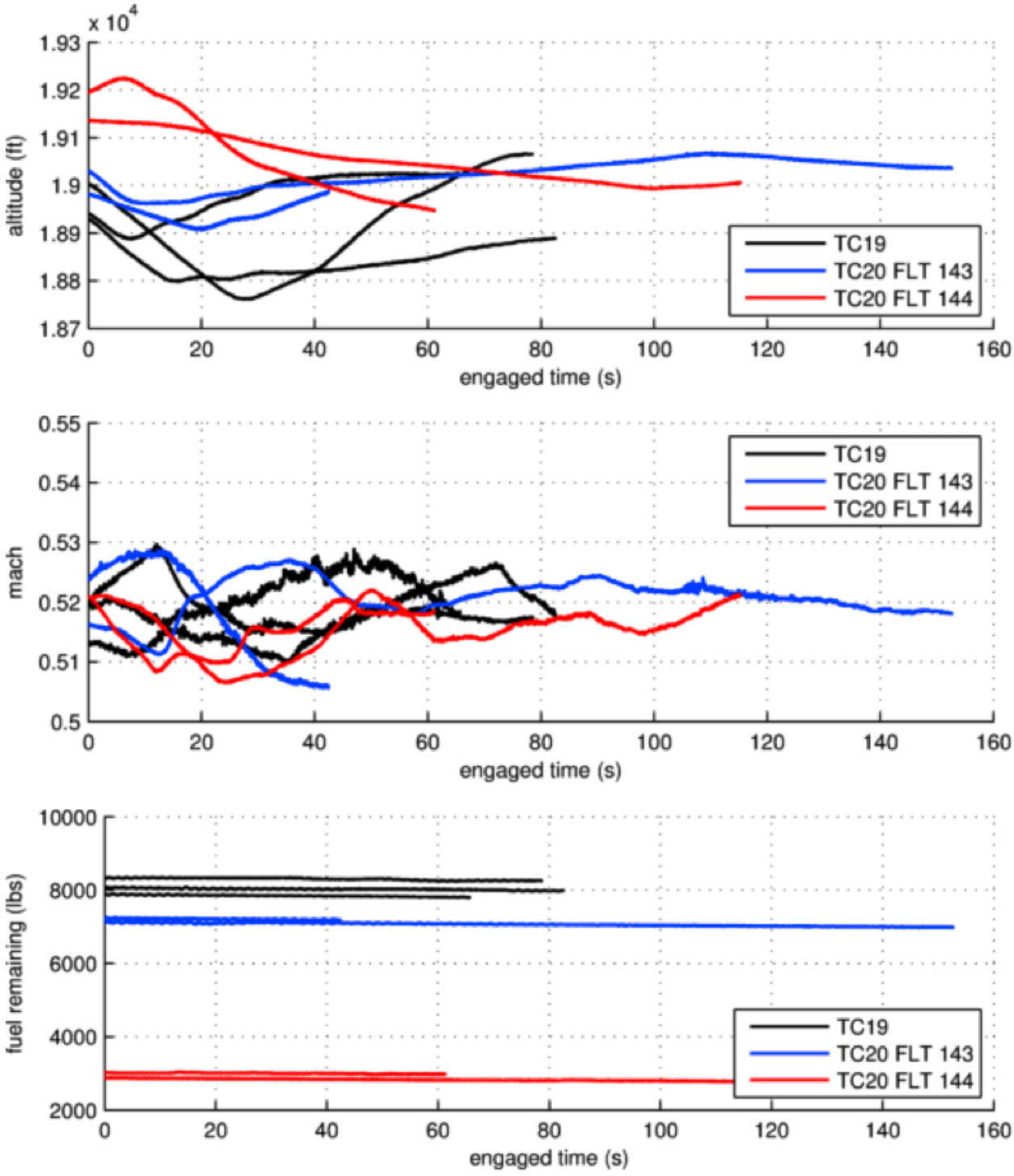

Figure 15. Test Case 20 Flight Conditions